Development 137, 519-529 (2010) doi:10.1242/dev.027045

The Engrailed homeobox genes determine the different foliation patterns in the vermis and hemispheres of the mammalian cerebellum

Yulan Cheng[1,†,*], Anamaria Sudarov[1,‡,*], Kamila U. Szulc[2], Sema K. Sgaier[1,§], Daniel Stephen[1], Daniel H. Turnbull[2] and Alexandra L. Joyner[1,¶]

SUMMARY

Little is known about the genetic pathways and cellular processes responsible for regional differences in cerebellum foliation, which interestingly are accompanied by regionally distinct afferent circuitry. We have identified the Engrailed (En) homeobox genes as being crucial to producing the distinct medial vermis and lateral hemisphere foliation patterns in mammalian cerebella. By producing a series of temporal conditional mutants in *En1* and/or *En2*, we demonstrate that both En genes are required to ensure that folia exclusive to the vermis or hemispheres form in the appropriate mediolateral position. Furthermore, *En1*/*En2* continue to regulate foliation after embryonic day 14, at which time Fgf8 isthmic organizer activity is complete and the major output cells of the cerebellar cortex have been specified. Changes in spatially restricted gene expression occur prior to foliation in mutants, and foliation is altered from the onset and is accompanied by changes in the thickness of the layer of proliferating granule cell precursors. In addition, the positioning and timing of fissure formation are altered. Thus, the En genes represent a new class of genes that are fundamental to patterning cerebellum foliation throughout the mediolateral axis and that act late in development.

KEY WORDS: Fgf8, Granule cells, Sonic hedgehog, Morphogenesis, En, Mouse

INTRODUCTION

A key question in developmental biology is how tissues acquire their overall shape, as proper tissue morphology underlies normal organ function. The anatomy of the cerebellum (Cb) exemplifies the relationship between differences in morphology and neural circuitry. In most vertebrates, the outer surface of the Cb folds during development creating mediolateral (ML) fissures surrounding folia (called lobules). The enlarged surface area created by the lobules allows for an increase in the number of neurons organized into a layered surface cytoarchitecture (called the cortex), and thus in the complexity of neural circuits and the range of behaviors controlled by the Cb. Whereas the Cb of most vertebrates has one foliation pattern along the ML axis, mammals have a central core, called the vermis, which has a foliation pattern that is distinct from the two surrounding hemispheres and the most lateral floculi-paraflocculi (Altman and Bayer, 1997). Furthermore, each region of the cerebellum receives distinct neural inputs. Most of the proprioceptive and sensory inputs project to the vermis, whereas the hemispheres are enriched with circuits arising from the cortex (Altman and Bayer, 1997; Purves et al., 2004; Sillitoe and Joyner, 2007). Moreover, in humans, compared with in mouse, the hemispheres are much larger than the vermis, possibly reflecting a greater cerebellum involvement in cortex-associated functions (Altman and Bayer, 1997; MacLeod et al., 2003). It is crucial to determine how the distinct morphology of each region is regulated during development.

Most mammals have a basic pattern of ten major lobules in the vermis (I-X anterior to posterior) and four in the hemispheres (Simplex, CrusI, CrusII and Paramedian). The foliation pattern rapidly transitions from the vermis to the hemispheres in the paravermis. The extent to which the major lobules are further subdivided by fissures varies between species (Larsell, 1970) and to a small degree between mouse strains (Inouye and Oda, 1980). There is a degree of continuity between the hemispheres and the vermis, as two of the vermis lobules (VI and VII) are continuous with the four lobules of the hemispheres. However, the morphology of the lobules is distinct in each ML region, and so is the degree of subdivision of the lobules. The genetic pathways that regulate the formation of distinct lobules in the vermis and the hemispheres are not known.

The Cb cortex consists of a dense layer of granule cells, an overlying monolayer of Purkinje cells and Bergmann glia, and an outer cell-sparse molecular layer (Goldowitz and Hamre, 1998). Although the Purkinje cells are derived from the ventricular zone of dorsal rhombomere 1 by embryonic day (E) 13.5 in mouse, the granule cells are generated from E18.5 to postnatal day (P) 16.5 by a progenitor layer covering the surface of the Cb (the external granule layer, EGL). Foliation occurs simultaneously with, and is dependent on, granule cell production (Lauder, 1974). At the base of each fissure, Purkinje cells and Bergmann glial fibers have a distinct cellular arrangement that could allow them to act as

[1]Developmental Biology Program, Sloan-Kettering Institute, 1275 York Avenue, New York, NY 10065, USA. [2]Structural Biology Program, Skirball Institute, New York University School of Medicine, 540 First Avenue, New York, NY 10016, USA.

*These authors contributed equally to this work
[†]Present address: Discovery Biology, Ernst Felder Laboratories, Bracco Research USA, Princeton, NJ 08540, USA
[‡]Present address: Laboratory of Neurogenetics and Development, Weill Medical College of Cornell University, New York, NY 10065, USA
[§]Present address: Bill & Melinda Gates Foundation, A-10, Sanskrit Bhawan, Qutab Institutional Area, Aruna Asaf Ali Marg, New Delhi 110067, India
[¶]Author for correspondence (joynera@mskcc.org)

Accepted 24 November 2009

'anchoring centers', so that proliferation of granule cells between anchoring centers would result in outward growth of lobules (Sudarov and Joyner, 2007). An important question is what genes regulate the formation of anchoring centers in the appropriate spatial and temporal manner to produce a normal foliation pattern.

Of the factors known to be required for Cb development, fibroblast growth factor 8 (*Fgf8*) is expressed from E8.5 to E12.5 by the isthmus organizer, and is required to specify the Cb primordium (Chi et al., 2003). Sonic hedgehog (Shh) secreted by the Purkinje cells after E16.5 is required to maintain granule cell precursor proliferation (Corrales, 2006; Lewis, 2004). By contrast, there is evidence that the two engrailed (En) homeobox transcription factors (Joyner and Martin, 1987) regulate the pattern of at least some lobules. In *En2* mutants, vermis lobule VIII is abnormally shifted posterior and only three lobules form in the hemispheres (Joyner et al., 1991; Millen et al., 1994). By contrast, *En1* null mutants on most genetic backgrounds are perinatal lethal and lack the cerebellum (Wurst et al., 1994; Bilovocky et al., 2003). However, when *En1* is conditionally ablated at ~E9, the Cb forms and some mutants ($En1^{lox/Cre}$) have normal foliation (Sgaier et al., 2007). These results raised the question of whether *En1* is required for the initial specification of the Cb primordium and *En2* is required subsequently for foliation. An alternative is that in $En1^{lox/Cre}$ mutants *En2* compensates for the lack of *En1* in foliation, as *En2* can replace *En1* in specification of the Cb (Hanks et al., 1995). Furthermore, lobules I-V and VIII are greatly reduced in size in $En1^{+/-}$; $En2^{-/-}$ mutants (Sgaier et al., 2007). The extent to which the two En genes regulate foliation throughout the ML axis of the Cb is not clear because of the early requirement for *En1* in specification of the Cb.

We produced a temporal series of *En2* and *En1/En2* conditional mutant mice and discovered that the two genes act together to preferentially promote formation of lobules that are specific to the hemispheres and the vermis. Furthermore, *En1/En2* are required even after *Fgf8* expression has ended for Cb foliation to be patterned normally. *En1/En2* regulate both the position and the timing of formation of fissures in the vermis. Also, the normal regional differences in the thickness of the EGL along the anteroposteior (AP) axis are altered in unison with changes in AP spatially restricted gene expression patterns. Thus, *En1/En2* are high in the genetic hierarchy that regulates the morphology of the entire Cb.

MATERIALS AND METHODS

Generation of mouse strains

All animal studies were performed under an approved IACUC animal protocol according to the institutional guidelines at the Memorial Sloan-Kettering Cancer Center (MSKCC). Gene targeting in ES cells (Matise et al., 2000) was used to generate mice containing $En2^{lox}$, $En2^{loxlz}$, $En2^{GFPloxIRES}$ and $Rosa26^{CreERT2}$ alleles (see Fig. S1 in the supplementary material). At least two targeted ES clones were identified for all the alleles by Southern blot analysis (data not shown) and injected into C57BL/6J blastocysts. Some chimeras were bred with *TK-Cre* (Bai et al., 2002) or *hACTB-Flpe* deleter mice (Rodriguez et al., 2000) to remove *neo* or to create a deleted allele. Mice were maintained on an outbred Swiss Webster background. The $En2^{lox}$ allele functions as wild type (WT), as $En2^{lox/-}$ mice are normal (Fig. 2C,D), and the deletion allele ($En2^{\Delta lox}$) as null, as $En2^{\Delta lox/\Delta lox}$ and $En2^{\Delta lox/-}$ mice display an $En2^{-/-}$ (Joyner et al., 1991) phenotype (data not shown; see Fig. 2F,G). $En2^{loxlz/loxlz}$ mice have a null phenotype and $En2^{\Delta loxlz/\Delta loxlz}$ mice appear normal (data not shown). The $En2^{GFPloxIRES}$ allele was found to express Gfp in the same pattern as En2 (data not shown) and to have a normal Cb when homozygous. The $En2^{GFPloxIRES}$ allele is hypomorphic, as $En1^{+/-}$; $En2^{GFPloxIRES/-}$ have a more extreme phenotype than do $En1^{+/-}$; $En2^{+/-}$ mice (see Fig. 3).

Tamoxifen administration, and genotyping

Noon on the day a vaginal plug was detected was designated as E0.5. Tamoxifen (TM) was administered by oral gavage to pregnant females at 17.00 hours on E9.5 or E10.5 (3.5-5 mg/40 g of body weight), or twice at 17.00 hours on E11.5 and E12.5 or E13.5 and E14.5 (4 mg + 3 mg). Genotyping was carried out using published PCR protocols (Joyner et al., 1991; Soriano, 1999; Sudarov and Joyner, 2007) or with modifications (see Fig. S1 in the supplementary material).

Histology, RNA in situ hybridization, β-galactosidase and immunohistochemistry analysis

Standard methods were used, and detailed protocols are available at http://www.mskcc.org/mskcc/html/75282.cfm. In general for histological analysis, 12-μm serial cryostat sections were obtained and analyzed at 96-μm intervals. The *Gli1* (Millen et al., 1995), *Fgf8* (Crossley and Martin, 1995), *Rnx* (Shirasawa et al., 2000) and *Otx2* (gift from J. Rossant, Hospital for Sick Children, Toronto) antisense RNA probes were as described previously. Bright-field images were collected using Magnafire or Volocity software. Fluorescent images were obtained with Openlab 3.5 or Volocity. The primary antibodies used were: rabbit anti-Enhb (Davis et al., 1991), mouse anti-BrdU (1:500; Becton Dickinson) and rabbit anti-Pax6 (1:1000, Chemicon). Secondary antibodies from Molecular Probes (donkey anti-rabbit, mouse IgG-Alexa488, donkey anti-rabbit IgG-Alexa555) were diluted 1:1000.

Quantification

To assay proliferation, pregnant females were administered 100 μg BrdU/g body weight 60 minutes prior to sacrifice. The percentage of BrdU-positive cells at E18.5 and P2 was calculated as the percentage of Pax6-positive cells that were also BrdU positive within the EGL below a 100 μm length (ImageJ software, NIH, was used to trace the length) of the outer surface at the top of lobules IV-V, or top of lobule VI. For E18.5 embryos, the three most medial sections (12 μm thick) and, for P2 animals, the six most medial sections were quantified from three brains each. The thickness of the EGL was calculated as the number of cell layers at the top of lobules IV-V and VI. A Student's *t*-test was performed for statistical analyses.

Magnetic resonance microimaging

Magnetic resonance microimaging (micro-MRI) was performed on a 7T micro-MRI (Bruker Biospec) with 750 mT/m actively shielded gradients (BGA09S, Bruker) using a 25-mm (i.d.) quadrature Litz coil (Doty Scientific) and a protocol modified from Johnson et al. (Johnson et al., 2002) (see movie legends in the supplementary material for details).

RESULTS

Strategy for time-specific activation of En2 or inactivation of En1/En2 function

As an approach to determine when the pattern of foliation is determined, an *En2* conditional knock-out (CKO) allele ($En2^{lox}$) was generated with loxP sites surrounding the homeodomain encoding region (see Fig. S1A in the supplementary material; Fig. 2A), as well as a hypomorphic conditional allele that expresses GFP and En2 before but only GFP after loxP-mediated deletion of exon 1 ($En2^{GFPloxIRES}$) (see Fig. S1B in the supplementary material). As a complement to temporal ablation, we generated an allele ($En2^{loxlz}$) in which *En2* function is silent until activated with Cre by inserting floxed *Tau-lacZ* sequences into the 5′ UTR of *En2* (see Fig. S1C in the supplementary material). We also generated a new *R26* (Zambrowicz et al., 1997) knock-in allele ($Rosa26^{CreERT2}$) that expresses the T2 form of *CreER* (Indra et al., 1999) with *neo* removed to ensure strong expression (see Fig. S1D in the supplementary material).

The recombination efficiency of our $R26^{CreERT2}$ allele was characterized using the $R26^{R}$ *lacZ* reporter allele (Soriano, 1999). X-galactosidase (X-gal) staining of sagittal sections of $R26^{CreERT2/R}$ embryos showed expression in most cells of the Cb when TM was

administered at E9.5 (Fig. 1A,B) or E10.5 (Fig. 1C,D), in many cells at E11.5 and E12.5 (Fig. 1E,F), and in a few cells at E13.5 and E14.5 (Fig. 1G,H). In adult brains of $R26^{CreERT2/R}$ embryos (TM on E10.5), β-gal activity was detected in all the major Cb cell types (Fig. 1K,L; data not shown). Efficient recombination was also detected in all other regions of the brain (data not shown). Importantly, no or only rare β-gal-expressing cells were detected in brains in the absence of TM (Fig. 1I,J).

To further assess recombination efficiency, En2 protein expression was analyzed in the adult Cb of *En2* conditional mutants, as En2 is expressed in most granule cells and in the interneurons within the molecular layer where En1 is largely absent (Davis et al., 1988; Millen et al., 1995) (see also Fig. 2E). In $En2^{lox/-}$;$R26^{CreERT2/+}$ mutants, quantitative analysis of recombination efficiency in interneurons of mutants with an *En2* null phenotype (n=2 for TM at E9.5, n=2 for TM at E10.5, n=2 for TM at E11.5 and E12.5) showed that compared with control mice, only ~10-30% of the interneurons expressed En2 in mutants (see Table S1 in the supplementary material) (compare Fig. 2E,H with 2K,N). Similarly, in $En2^{loxlz/loxlz}$;$Rosa26^{CreERT2/+}$ mutants treated with TM on E10.5, or on E11.5 and E12.5, recombination efficiency was high (up to 88%) (Fig. 2Q; data not shown), indicating a broad restoration of *En2*

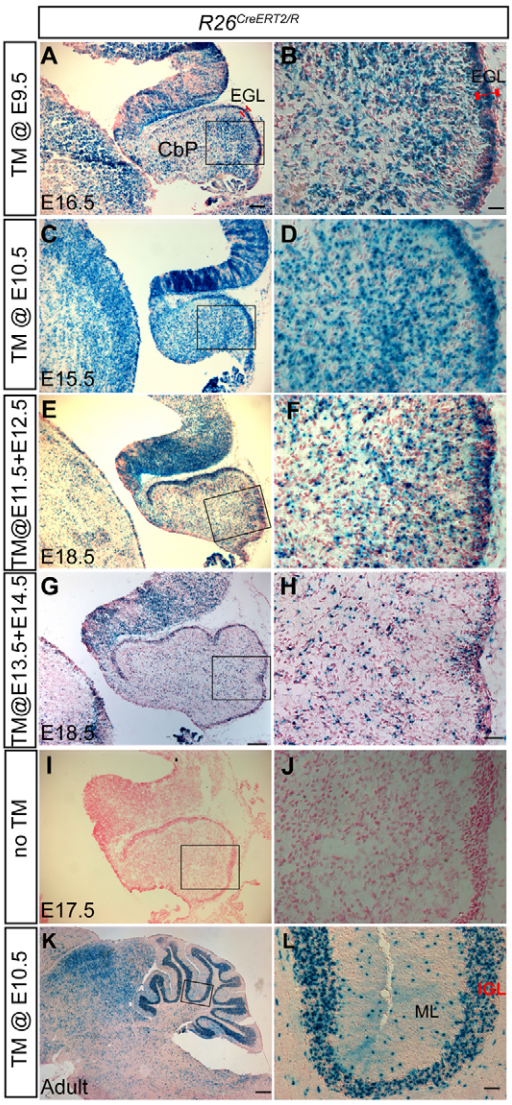

Fig. 1. The *Rosa26*^{CreERT2} allele produces efficient recombination in the embryonic brain until late gestation. (**A-L**) X-galactosidase staining of Cb sagittal sections of $Rosa26^{CreERT2/R}$ embryos (A-J) or adults (K,L) treated with tamoxifen (TM) at the times indicated. Panels on right are higher powerered images of the areas outlined in the left panels. Anterior is to the left. Scale bars: 100 μm in A,C,E,G,I; 25 μm in B,D,F,H; 400 μm in K; 50 in μm L.

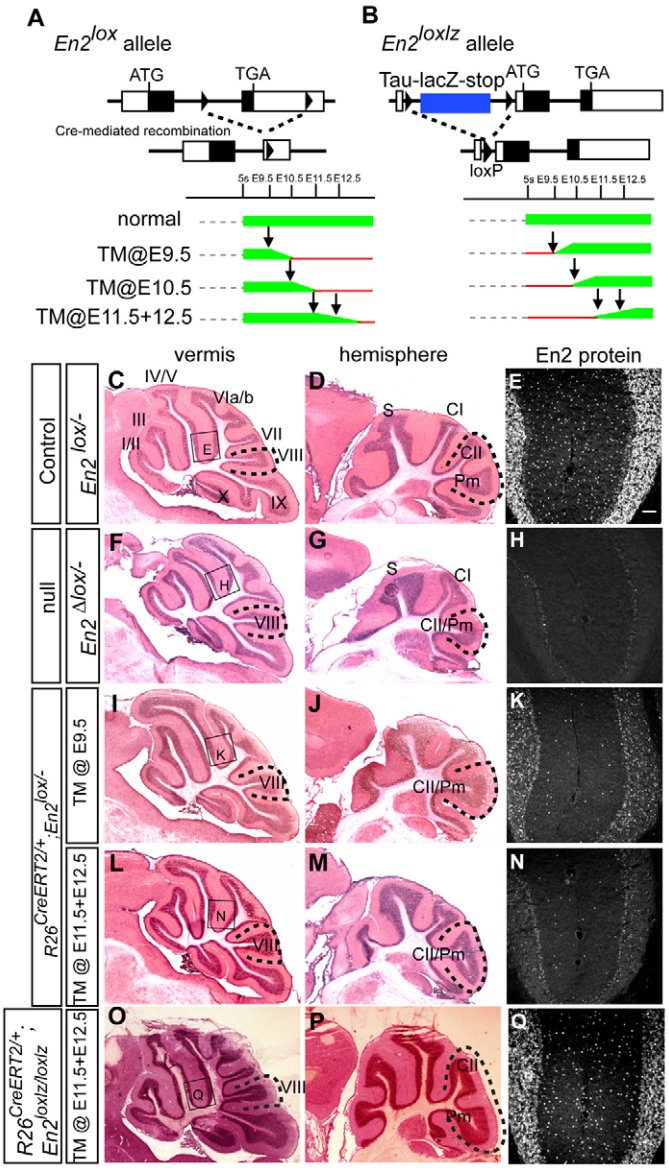

Fig. 2. *En2* is required after ~E12 to regulate the Cb foliation pattern. (**A**,**B**) Schematics (not drawn to scale) of conditional $En2^{flox}$ (A) or $En2^{floxlZ}$ conditional (B) alleles and the corresponding experimental time-course used to ablate or activate *En2*, respectively. Green rectangles and red lines represent the periods when *En2* was expressed or ablated, respectively; arrows indicate the time of TM administration. Hematoxylin and Eosin (H&E)-stained sagittal sections are shown of the vermis (**C**,**F**,**I**,**L**,**O**) and hemispheres (**D**,**G**,**J**,**M**,**P**) of the mutants indicated. Inactivation of *En2* up to ~E12 produces an *En2* null mutant phenotype, whereas activation at ~E12 rescues the foliation defects. (**E**,**H**,**K**,**N**,**Q**) Images of immunostaining for En2 protein in the boxed vermis regions. Defective folia are outlined by dotted lines. S, Simplex; CI, CrusI; CII, CrusII; Pm, Paramedian. Scale bar in E: 200 μm for C,D,F,G,I,J,L,M,O,P; 25 μm for E,H,K,N,Q.

expression. To further assess the timing of functional ablation, we performed western blot analysis and analyzed the initiation of molecular and morphological phenotypes. Analysis of En2 protein in brain extracts from $En2^{lox/-};R26^{CreERT2/+}$ compared with $En2^{-/+}$ and $En2^{+/+}$ control embryos showed that a decrease in protein was apparent at 36 hours (n=2) post-TM treatment at E10.5, and at 72 hours En2 was barely detectable in mutants (see Fig. S2 in the supplementary material). Furthermore, the Cb primordium was reduced in size and *Fgf8* expression decreased by 48 hours post-TM treatment at E10.5 in *En1/En2* double CKOs (see below). We conclude that functional ablation of *En1/En2* occurs around 36 hours after TM treatment and thus designate gene ablation as ~36 hours post-TM.

En2 is required after ~E12.5 to regulate patterning of folia

We first addressed whether *En2* is required for foliation during the time the Cb primordium is being generated (prior to E13.5). Unlike the wild-type foliation pattern (Fig. 2C,D) seen in some $En1^{lox/Cre}$ mutants, all $En2^{lox/-};Rosa26^{CreERT2/+}$ CKO embryos administered TM on E9.5 (*En2-E9.5* CKO, n=3) had a phenotype similar to that of *En2* null mutants (Fig. 2F,G,I,J). Furthermore, when TM was administered later than E9.5, most of the *En2* CKO mutants (2/3 for TM at E10.5; 3/4 for TM at E11.5 and E12.5) displayed a foliation pattern similar to that of *En2* null mutants (Fig. 2L,M ; data not shown). Thus, *En2* is required for Cb foliation after ~E13.

We next activated *En2* function at different developmental time points using our $En2^{loxlz}$ allele to investigate whether *En2* is dispensable prior to ~E13. Indeed, the adult hemisphere Cb foliation pattern of all $Rosa26^{CreERT2/+};En2^{loxlz/loxlz}$ mice (9/9) and the vermis of the majority of mice (2/3 for TM at E9.5, 3/4 for TM at E10.5, 1/2 for TM at E11.5 and E12.5) was rescued compared with in $En2^{loxlz/loxlz}$ mice and resembled that of the wild type (Fig. 2O,P). Thus, *En2* is required for Cb foliation after ~E13.

En1 and *En2* act together after E11 to produce diversity in foliation in the vermis and hemispheres

Although *En1* is not required after E9 for Cb foliation in the presence of two normal *En2* alleles, it is possible that *En1* and *En2* act together after this time point to regulate foliation, and that patterning of the entire Cb is dependent on both genes. We therefore analyzed *En1/En2* double CKOs on a double heterozygous background in which only some animals have a mild anterior foliation defect (Sgaier et al., 2007). Strikingly, sagittal sections (n=4) or micro-MRI imaging (n=1) of the Cb of the *En1/2-E10.5* CKO mutants that survived past P13 revealed that neither the vermis nor the hemisphere foliation patterns resembled those of controls ($Rosa26^{CreERT2/+};En1^{lox/+};En2^{lox/+}$ mice treated or not treated with TM; see Fig. 3A,B, Fig. 4; data not shown) or $En2^{-/-}$ mice. *En1/2-E9.5* CKOs died at birth and had a major deletion of the midbrain and medial Cb (data not shown), which is likely to be due to the early requirement for *En1/En2* in specification of the Cb primordium.

We took two approaches to determine the nature of the lobules remaining in the mutants. Photographs of a sagittal series of sections were examined for each mutant (see Fig. S3 in the supplementary material), and 3D reconstructed micro-MRI images of a P14 *En1/2-*

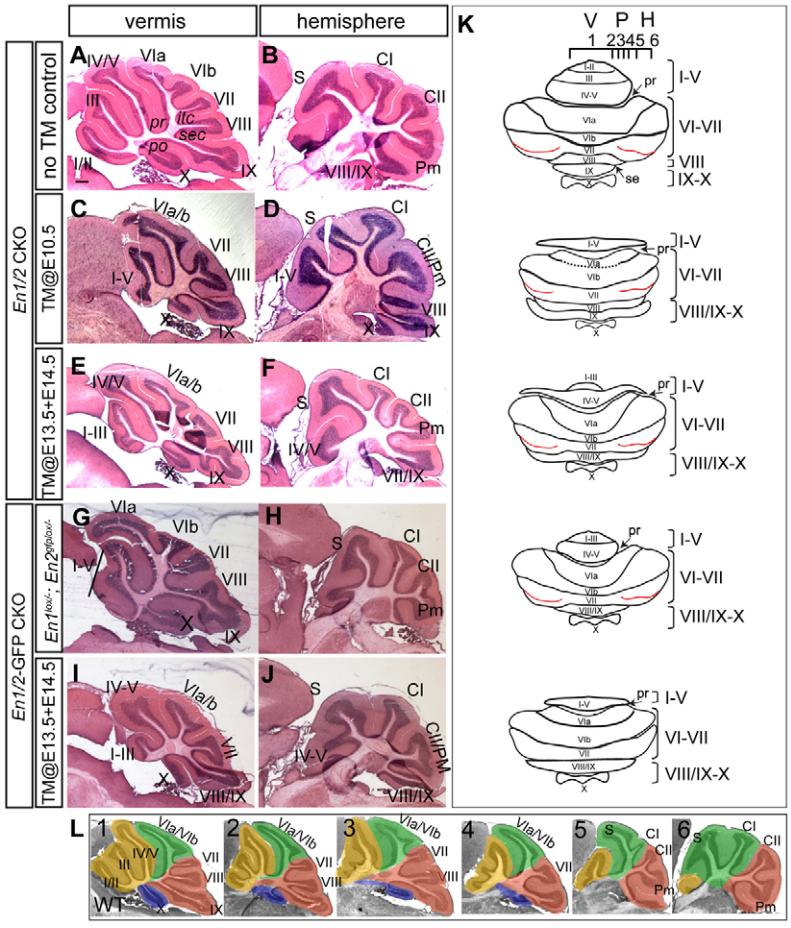

Fig. 3. Inactivation of both *En1* and *En2* preferentially affects the lobules specific to the vermis and the hemispheres. (**A-J**) H&E-stained sagittal sections of adult Cb from the mutants indicated. (**K**) Schematics of idealized surface renderings of foliation of a flattened Cb based on sections and micro-MRI of all mutants. (**L**) A series of medial to lateral sagittal sections of adult wild-type (WT) Cb are shown with shading of lobules I-V (yellow), VIa-b (green), VI-IX (red) and X (blue). The earlier *En1/En2* expression is removed, lobule I-V and VIII in the vermis are reduced in size, remnants of lobules I-V and VIII/IX are extended more laterally than normal, lobules VI/VII in the vermis are relatively larger than normal, and CII and Pm in the hemispheres are fused. Scale bar: 200 μm.

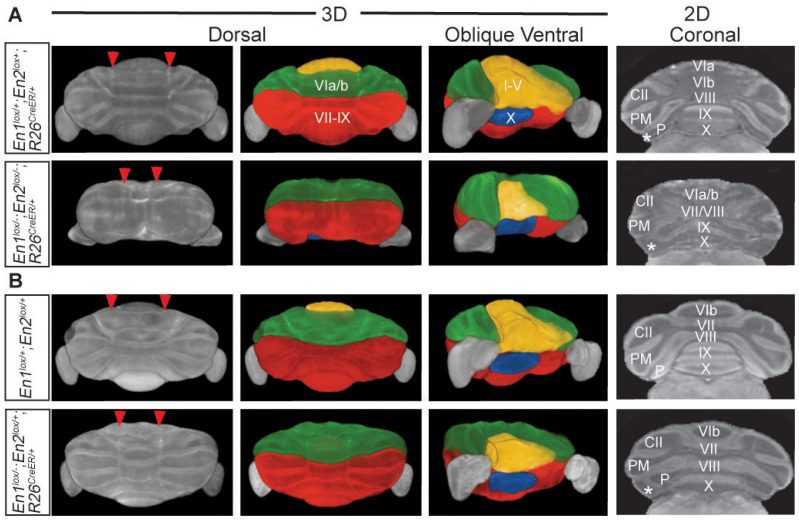

Fig. 4. Inactivation of both *En1* and *En2* produced a more homogeneous foliation pattern along the ML axis. Volumetric micro-MRI data was used to generate dorsal and oblique ventral (3D) views of surface rendered images, as well as coronal sections (2D) of the cerebellum at P14 (**A**) and P21 (**B**). Coloring is as in Fig. 3. Arrowheads indicate approximate morphological borders between vermis and hemispheres (dorsal views); asterisks indicate lateral extension of posterior lobules in mutants (coronal sections). All mice analyzed with micro-MRI were treated with TM at E10.5.

E10.5 CKO and P21 *Rosa26*$^{CreERT2/+}$;*En1*$^{lox/-}$;*En2*$^{lox/+}$ mutant and littermate controls were analyzed (Fig. 4; see also Movies 1-4 in the supplementary material). In wild-type mice, the vermis has nine or ten lobules depending on the strain, with lobules I and II being fused in most strains, including in the outbred background used in these studies. Lobules I-V, referred to as the anterior vermis, do not extend into the hemispheres (yellow, Fig. 3L). The central vermis consists of lobules VI and VII, which are continuous with the hemisphere lobules. In many strains, lobule VI is divided by a shallow fissure into two sublobules called VIa and VIb (green, Fig. 3L). Sublobule VIa is continuous with lobule Simplex in the hemispheres, lobule VIb with CrusI, and lobule VII with CrusII and Paramedian. Lobule VIII in the posterior vermis diminishes in size as it extends laterally (called the copula pyramidis in the hemispheres), and lobules IX and X do not extend into the hemispheres (blue, Fig. 3L).

Based on the examination of a series of histological sections and micro-MRI images of the Cb, only the most posterior lobule of *En1/2-E10.5* CKO mutants had a normal appearance; this was therefore designated as lobule X. The three vermis lobules anterior to lobule X had a very abnormal morphology for this region of the vermis (red in Fig. S3 and Movie 2 in the supplementary material). We designated these lobules as VII, VIII and IX, as lobule VII was continuous with CrusII/Paramedian in the hemispheres. Lobule VIII and IX fused laterally in most mutants and extended more laterally than normal (Fig. 4, asterisks in 2D coronal images). The adjacent vermis lobule was continuous with the anterior two lobules of the hemispheres, Simplex and CrusI (green in Fig. S2 and Movie 2 in the supplementary material), and was therefore designated as lobule VIa/b in the vermis. The remaining anterior-most 1-2 lobules in the vermis of *En1/2-E10.5* CKO mutants were designated as lobules I-V but, interestingly, unlike in wild type, the remnants of lobules I-V extended into the hemispheres (yellow in Fig. S2 and Movies in the supplementary material). Furthermore, in the *Rosa26*$^{CreERT2/+}$;*En1*$^{lox/+}$;*En2*$^{lox/+}$ P14 double heterozygous control, lobule VIII extended more laterally than normal, as did lobules I-V, but only on one side (Fig. 4; see also Movie 1 in the supplementary material).

The hemispheres of *En1/2-E10.5* CKO mutants had a more complex morphology than normal, as they maintained remnants of the vermis-specific anterior and posterior regions more laterally than normal. In addition, in some mutants lobule VIII was diminished more medially than lobule IX, rather than the opposite as occurs in wild type. Thus, when *En1/En2* function is reduced after ~E12, the vermis and hemisphere morphologies converge towards an intermediate foliation pattern. Consistent with the foliation pattern being more homogeneous along the ML axis than normal, in the surface renderings of the P14 *En1/2-E10.5* CKO Cb the normally clear distinction between the vermis and the hemispheres was not apparent (Fig. 4; Fig. 3D, dorsal images).

A striking aspect of the vermis phenotype is that the anterior region (lobules I-V) appeared to be preferentially reduced and the central region (lobules VI-VII) preferentially expanded. To determine whether this is the case, we used the 3D micro-MRI image data sets for a volumetric analysis of mutant and control brains by segmenting out lobules I-V, VI-VII, VIII-IX and X in the vermis, and calculated their volume. Indeed, we found that whereas in the control Cb lobules I-V occupy 44% of the volume of the vermis, in the P14 *En1/2-E10.5* CKO mutant they only occupied 24% (Table 1). Furthermore, lobules VI-VII occupied a greater proportion of the vermis in the *En1/2-E10.5* CKO than in the control (52% compared with 19%), whereas lobules VIII-IX occupied less (15% in mutant compared with 29% in control). Lobule X occupied the same volume of the vermis in the mutant and the wild-type cerebellum (8% and 9%, respectively). This same trend in changes in the relative volumes of specific lobules within the vermis was apparent in the *Rosa26*$^{CreERT2/+}$;*En1*$^{lox/-}$;*En2*$^{lox/+}$ mutant, which has a milder phenotype (Table 1).

En1/En2 are required for robust expression of *Fgf8* in the isthmic organizer after E11

One possible contributing factor to the reduction in size of anterior lobules in the medial Cb of *En1/2*-E10.5 CKO mutants is a reduction in *Fgf8* expression, as mutants with reduced Fgf8 signaling have fewer anterior lobules (Xu et al., 2000; Basoon et al., 2008; Sato et al., 2009) and *Fgf8* expression is lost by E9.0 in *En1/En2* double null mutants (Liu and Joyner, 2001). To determine whether *En1/En2* are required to maintain *Fgf8* expression, we examined *Fgf8* expression in *En1/2*-E10.5 CKO mutants. Indeed, *Fgf8* expression was reduced specifically in the dorsal midline at E12.5 (Fig. 5A-D). In addition, the Cb primordium was reduced in size. By contrast, the midbrain gene *Otx2*, which is negatively regulated by *Fgf8* (even when *Fgf8* is eliminated after E10.5) (Sato et al., 2009), and which can convert the hindbrain into a midbrain (Broccoli et al., 1999), was not expanded posterior in the dorsal

midline (Fig. 5E,F). Thus, *En1/En2* are required to maintain full expression of *Fgf8* after ~E11, but the Cb primordium is not converted into a midbrain phenotype in *En1/En2* CKOs.

En1 and *En2* regulate vermis foliation after *Fgf8* expression ends

As an approach to determine whether the decrease in *Fgf8* expression alone accounts for the reduced size of lobules I-V, and to further explore when *En1/En2* are required for patterning foliation, we reduced the activity of *En1/En2* after *Fgf8* is expressed in the isthmus. In adult *En1/2-E13.5+E14.5* CKO mutants (n=2), the vermis had a foliation pattern that was a milder version than that observed in the *En1/2-E10.5* CKO mutants (compare Fig. 3E with 3L3; see also Fig. S2 in the supplementary material). In the anterior region, lobules IV/V were present and lobules I-III were fused into one lobule, and in the posterior region lobule VIII was shifted posterior and fused with dorsal lobule IX. The hemisphere foliation pattern appeared similar to that of wild type except that lobules I-V and VIII/IX of the vermis were present more laterally than normal (Fig. 3F; Fig. S2 in the supplementary material).

To further test the requirement for *En1/En2* in regulating foliation after ~E15, we took advantage of our hypomorphic $En2^{GFPloxIRES}$ allele to provide a genetic background further depleted for *En1/En2*. In the vermis of $En1^{lox/-};En2^{GFPloxIRES/-}$ control mice, only one or two major anterior lobules were present, and lobule VIII was very small and fused with dorsal lobule IX (Fig. 3G). In the hemispheres, CrusII and Paramedian were only partially separated (Fig. 3H). As expected, $En1/2^{GFP}$*-E13.5+E14.5* mutants ($Rosa26^{CreERT2/+};En1^{lox/-};En2^{GFPloxIRES/-}$ treated with TM) had a more extreme phenotype in both the vermis and the hemispheres (Fig. 3I,J). In summary, *En1/En2* are required independently of Fgf8 isthmic organizer activity and after at least ~E15 to promote the distinct foliation patterns in the vermis and the hemispheres.

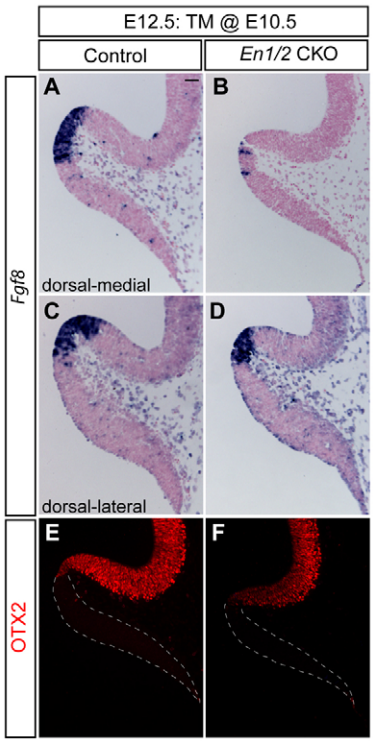

Fig. 5. *En1/En2* are required for robust expression of *Fgf8* in the isthmic organizer after ~E11. (**A-D**) Medial (A,B) and slightly lateral (C,D) sagittal sections showing that *Fgf8* RNA expression is reduced in the dorsal medial mid/hindbrain junction at E12.5 in *En1/2-E10.5* CKOs compared with in controls. (**E**,**F**) Expression of Otx2 protein does not extend into the hindbrain in mutants. Cb primordium is outlined with a white dotted line. Scale bar: 25 μm.

En1/En2 regulate the order in which fissures form

We recently demonstrated that lobule VIII is smaller and shifted posteriorly in *En2* mutants, because the fissure separating lobule VIII from lobule IX (secondary, se) forms later than normal, producing a shallower fissure, whereas the fissure between lobules VIII and VII (prepyramidal, ppy) forms earlier than normal creating a deeper fissure (Sudarov and Joyner, 2007). This is in contrast to mutants in which there is a general decrease in granule cell proliferation or an increase in cell death, as the formation of fissures is delayed but the order in which they form is normal and in extreme mutants the last fissures do not form (e.g. Corrales et al., 2006). We therefore tested whether the timing of fissure formation in the vermis of *En1/En2* temporal CKO mutants correlated with the altered foliation pattern in adults.

In our control mice, each fissure in the vermis formed in a reproducible temporal series, with the preculminate (pcu), primary (pr) and se fissures forming almost simultaneously at E17.5 to divide the cerebellum into lobules I-III, IV/V and VI-X, followed by formation of the most posterior fissure (posterolateral, po), which separates lobule X from IX, by E18.5 (Fig. 6A). The ppy fissure then formed by P1 to separate VIII from VI/VII, followed by the precentral (pct) fissure separating lobules I/II from III by P2, the

Table 1. Comparison of regional volumes of the cerebellum when TM is administered at E10.5

	P14 % volumes		P21 % volumes	
	$En1^{lox/+};En2^{lox/+};R26^{CreER/+}$	$En1^{lox/-};En2^{lox/-};R26^{CreER/+}$	$En1^{lox/+};En2^{lox/+}$	$En1^{lox/-};En2^{lox/-};R26^{CreER/+}$
	% of brain			
Cerebellum	12	9	13	13
	% of Cb			
Vermis	27	28	29	27
Hemispheres	59	65	59	61
fl-pfl	14	7	12	12
	% of vermis			
Lobules I-V	44	24	40	33
Lobules VI-VII	19	52	25	38
Lobules VIII-IX	29	15	28	22
Lobule X	8	9	7	8

intercrural (itc) fissure (dividing lobules VIb/VII) and then, finally, the superior posterior (sp) fissure (dividing lobules VIa/VIb; see Fig. 6D,G, Fig. 7C). By contrast, the fissures in the hemispheres that are continuous with sp and itc in the vermis form nearly simultaneously by P1 (Fig. 6A′,D′), and the hemisphere-specific ansoparamedial (ans) fissure separating lobule CrusII from Paramedian forms much later (~P5) (Millen et al., 1994). In the paravermis, the itc, ppy and se fissures form by P1 (after the pr, pcu and po fissures; Fig. 6J).

Like mutants with a general defect in the production of granule cells, we found that *En1/En2* temporal CKO mutants had a smaller Cb and a delay in fissure formation, and that the delay was progressively longer as the phenotype worsened (Fig. 6). However, unlike mutants with a general granule cell defect, the order of fissure initiation was altered in *En1/En2* temporal CKOs. We concentrated on analyzing the vermis, as it was not possible to determine the position of the primordia of the paravermis and hemispheres in mutants. To identify the vermis fissures, and thus the intervening lobules, in *En1/2-E10.5* CKOs, we analyzed the expression of markers with restricted expression domains along the AP axis of the developing vermis. Strong expression of *Otx2* in the external granule layer (EGL) of control mice marks lobules IX and X (Frantz et al., 1994) (Fig. 7E,G). Thus, the anterior border of *Otx2* expression demarcates the se fissure. *Rnx* (Shirasawa et al., 2000), by contrast, is expressed strongly in the EGL of lobules VII-IX (Fig. 5I,K), and thus demarcates the po fissure posteriorly and the itc fissure anteriorly. We found that the *Otx2* and *Rnx* expression domains had similar relative positions in *En1/2-E10.5* CKO mutants at E18.5 and P2 (Fig. 7E-L), although the relative size of the domains was altered (see below). Based on the borders of *Otx2* and *Rnx* expression in *En1/2-E10.5* CKOs, the two fissures that are present at P2 are the pr and the itc (Fig. 7L). The se and po fissures then form by P3 (Fig. 6H). However, interestingly, the pr fissure is deeper than the itc fissure at P3, consistent with the greater depth of the pr fissure in adult mutants. The order of fissure formation in the *En1/2-E10.5* CKO vermis is therefore more similar to the lateral positions in the wild-type Cb, although formation of the ppy fissure is delayed (Fig. 6J,K). Thus, *En1/En2* regulate the temporal sequence by which fissures form throughout the vermis, and the changes seen in *En1/En2* mutants are likely to contribute to the altered adult foliation pattern.

En1/En2 regulate the position at which fissures form along the AP axis

To determine whether the change in the relative volumes of lobules seen in the adult vermis are present when foliation first initiates in the *En1/2-E10.5* CKOs mutants, or whether the changes develop later, we measured the length of the outer surface of lobules I-V, VI, VII-IX and X at P2 and in the adult. In the P2 mutants, lobules I-V represented only 22% of the P2 midline Cb compared with 46% for the wild type (Fig. 7U), similar to lobules I-V encompassing 24% and 44% of the P14 mutant and control vermis, respectively (Fig. 7U). The length of the outer surface of lobule X in the mutants occupied a similar percentage of the Cb as in the wild type at P2 (~8%). In addition, lobule VI was much larger than normal in P2 *En1/2-E10.5* CKOs (30.6% length in the mutant compared with 13.6% for the wild type), and lobules VI-IX were slightly larger in the mutants (Fig. 7U). Similar alterations in the proportion of the volume of the vermis occupied by each region were observed in the P14 *En1/2-E10.5* CKOs (Fig. 7U). Thus, in *En1/En2* mutants, although the relative positions of the domains of AP markers are preserved in the vermis, the relative sizes of the domains are changed, correlating with an alteration in the positioning of fissures along the AP axis. Therefore, *En1/En2* regulate both the timing of fissure formation and their position along the AP axis.

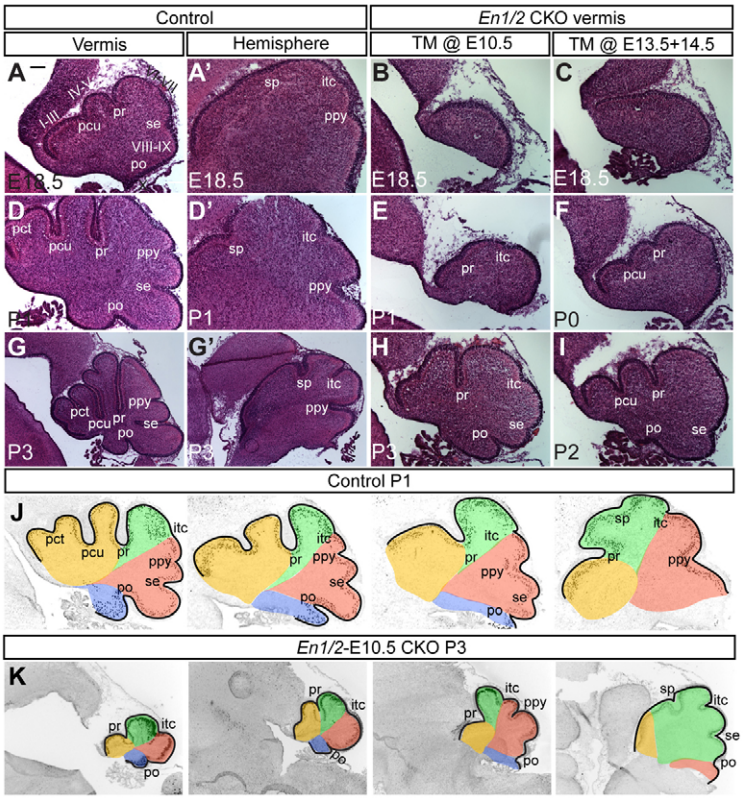

Fig. 6. *En1/En2* determine the timing of fissure formation. (**A-I**) H&E staining of vermis and hemisphere sagittal sections of the developing Cb in the mutants indicated compared with controls. (**J**,**K**) Outlines of a medial-to-lateral (left to right) series of sagittal sections of P1 wild type (J) and P3 *En1/2-E10.5* CKOs (K) illustrate foliation pattern. Regions highlighted as in Fig. 3L. Scale bar in A: 100 µm for A-F,H,I; 25 µm for G,G′.

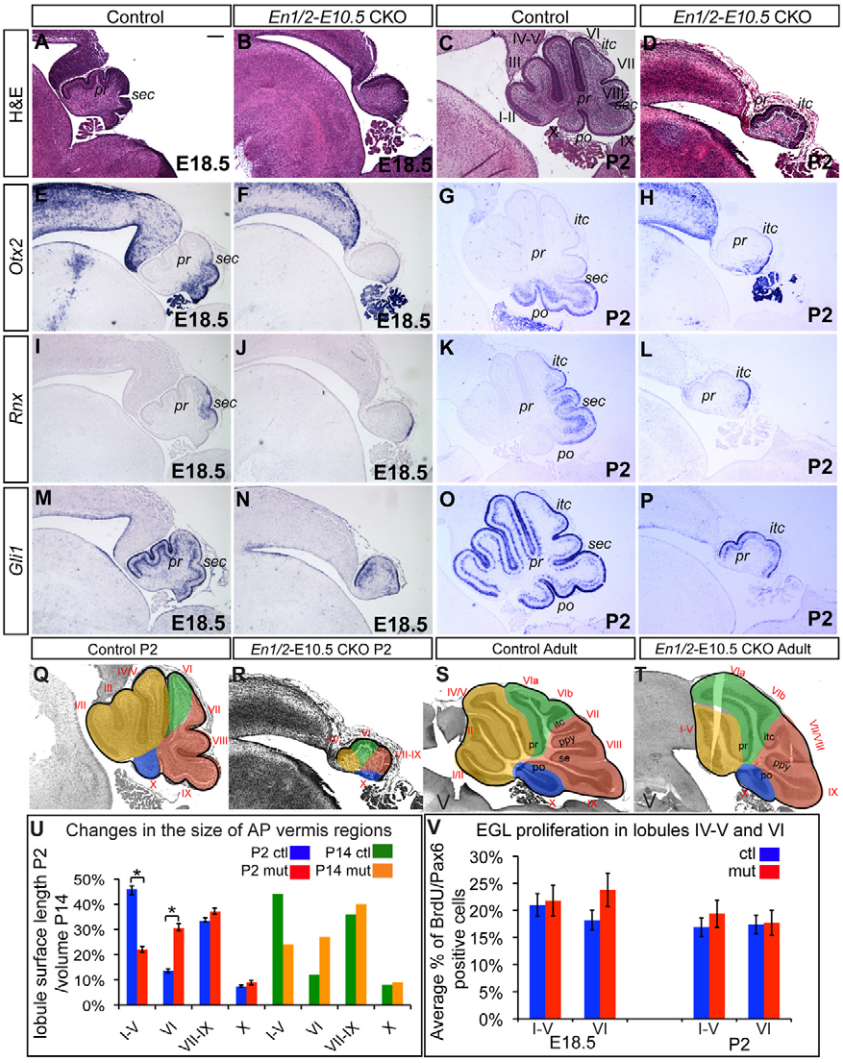

Fig. 7. Regional markers reveal that AP patterning of the Cb is altered at ~E18.5, prior to fissure formation in *En1/2* CKOs. (**A-P**) H&E staining (A-D) and RNA in situ hybridization of sagittal sections through the vermis of controls (*R26*$^{CreER/+}$; *En1*$^{+/lox}$; *En2*$^{+/lox}$) and *En1/2-E10.5* CKOs showing *Otx2* (E-H), *Rnx* (I-L) and *Gli1* (M-P) expression. (**Q-T**) Outlines of sagittal sections of P2 or adult brains shaded as in Fig. 3L to illustrate the relationship between lobules at two stages. (**U**) Graph comparing lengths of surface of the Cb at P2 and volumes at P14 of different lobules. **P*<0.0001. (**V**) Percentage of BrdU- and Pax6-positive cells in the EGL (Pax6^{+}) is shown graphically for the top of lobule VI-V compared with the top of VI at E18.5 and P2. Scale bar: 200 μm.

En1/En2 regulate regional gene expression and EGL thickness prior to and during foliation

We next examined the molecular and cellular basis of the changes in foliation at E18.5 and P2 in *En1/2-E10.5* CKOs. Surprisingly, at E18.5 prior to the initiation of foliation in *En1/2-E10.5* CKOs, *Otx2* and *Rnx* were nevertheless expressed in regionally restricted domains, similar to at P2 (Fig. 7F,J). In the wild-type cerebellum at E18.5 and P2, the absence of the itc and ppy fissures in the region of lobules VI and VII is accompanied by a thinner EGL compared to in the region encompassing lobules I-V (Altman and Bayer, 1997; Corrales et al., 2004). We therefore investigated whether the delay in foliation in *En1/2-E10.5* CKOs is associated with a general thinning of the EGL, and whether the relatively earlier foliation in the central region of the mutants compared to the anterior region is accompanied by a change in the relative thickness of the EGL in the two regions. The expression domains of *Rnx* and *Gli1* (see below) were used as landmarks to identify the presumptive lobules I-V and VI in mutants. Whereas the wild-type EGL at E18.5 was much thicker at the top of lobules IV/V than lobule VI (top of lobule VI/VII contained ~30% less cells than the top of IV), in *En1/2-E10.5* CKOs the EGL thickness was more similar in the two regions (the top of lobule VI contained ~15% less cells than the top of I-V; see Table 2). Curiously, the thickness of the EGL was 1.5-2 times greater in the mutants than in wild types at E18.5 (Table 2), although the overall size of each region, and thus total number of cells, was greatly reduced in the mutants. At P2 in the controls, the EGL at the top of lobule IV/V continued to be thinner than in lobule VI by ~25%, but it had nearly doubled in thickness in both regions (Table 2). Strikingly, in the *En1/2-E10.5* CKOs at P2 the EGL thickness was similar to at E18.5 and thinner than in the controls. The difference in thickness of the mutant EGL at the top of lobule VI compared to at the top of lobules I-V was ~22%. Thus, the relative thickness of the EGL in the anterior and central regions of the Cb were more similar to each other in *En1/2-E10.5* mutants than in wild type, and the overall thickness was greater in the mutants at E18.5 but thinner by P2 compared with in controls.

We next sought to determine whether the differences in EGL thickness are due to differences in the percentage of granule cells proliferating (see Fig. S4A-F in the supplementary material). The percentage of BrdU positive (proliferating) cells in the EGL [Pax6+ cells (Engelkamp et al., 1999)] in the controls at E18.5 tended towards being slightly higher at the top of lobules IV/V (~21.0%) than at the top of lobule VI (~18.2%). By contrast, in the *En1/2-E10.5* CKOs the opposite trend was seen (21.8% at the top of lobules I-V compared with 23.8% at the top of lobule VI; Fig. 7V). If the total number of cells in each region is taken into account, then in the wild type there were more proliferating cells per 100 μm of Cb surface in the anterior lobules than in the central lobules, and a more

Table 2. Changes in growth of the EGL in *En1/2-E10.5* CKO mutants around birth

	E18.5*				P2*			
	$En1^{lox/+};En2^{lox/+}$		$En1^{lox/-};En2^{lox/-};R26^{CreER/+}$		$En1^{lox/+};En2^{lox/+};R26^{CreER/+}$		$En1^{lox/+};En2^{lox/+};R26^{CreER/+}$	
EGL	IV/V	VI	IV/V	VI	IV/V	VI	IV/V	VI
Cell number†	43.65±3	31.3±2	65.1±7	55.9±1	84.1±10	64.9±10	64.3±5	50.4±4
	$P<0.0001$		$P<0.71$		$P<0.004$		$P<0.003$	
VI/IV-V‡	71.9%		84.9%		74.6%		78.2%	
Thickness§	4-6	2-3	7-11	4-6	6-9	3-6	4-6	3-5

*All mice were treated with TM on E10.5.
†Cell number, average number of $Pax6^+$ cells per 100 μm outer surface of the EGL.
‡VI/IV-V%, average percentage of the cell number in lobule VI compared with lobules IV-V.
§Thickness, range of cell layers in 100 μm outer surface of the EGL.

similar total number in the two regions of the mutants. At P2, the percentage of BrdU-positive EGL cells in wild-type and mutant mice was more similar in the two regions than at E18.5 (Fig. 7V).

Finally, since Shh stimulates granule cell proliferation after E17.5, we investigated whether Shh signaling was altered in *En1/2-E10.5* CKOs (n=3) compared with in wild types (n=3) by analyzing expression of the direct target gene *Gli1* (Bai et al., 2002). Interestingly, as in wild types, *Gli1* expression was detected in *En1/2-E10.5* CKOs (n=3) at E18.5 and there was a slight reduction in the level of *Gli1* in the central region, between the pr and sec fissures present in the wild type (Fig. 7M,N). Interestingly, consistent with the change in the relative sizes of the anterior and central regions in mutants, the region with lower expression in mutants comprised a larger percentage of the total length of the surface of the Cb compared with controls (9.3% in controls compared with 26.3% in mutants). At P2, *Gli1* expression in the EGL was more even along the AP axis in both the controls and mutants, with a slight decrease anterior to the itc fissure. Thus, a delay in the initiation of Shh signaling does not appear to account for the overall smaller size of the Cb at E18.5 or later in *En1/2-E10.5* CKOs, but the relative sizes of the regions of high and low expression of *Gli1* at E18.5 change in unison with the subsequent change in foliation pattern.

DISCUSSION

En1 and *En2* function together to regulate Cb foliation late in embryogenesis

Our use of temporal conditional mutagenesis to circumvent the early requirement for *En1* in specifying the Cb not only uncovered a greater degree of overlapping function between *En1* and *En2* in regulating Cb foliation than was possible using null mutants, but also provided insight into when each gene is required for foliation (Table 3). Unlike *En1*, *En2* continued to be required after E9 for foliation (Fig. 2). Analysis of double *En1/En2* CKO mutants compared with single CKOs uncovered a later requirement for the two En genes working together to regulate Cb foliation than for either gene alone. Although mosaic deletion of *En2* alone after ~E14 resulted in no foliation defect (data not shown), when the two genes were knocked down after ~E15 the vermis foliation pattern was severely altered. Thus, our study demonstrates that the pattern of lobules is regulated after the Purkinje cells and neurons of the deep cerebellar nuclei are born and granule cell specification is initiated. Consistent with this, we observed changes in spatially restricted gene expression and EGL thickness after E15 in *En1/2-E10.5* CKOs.

Our finding that the phenotype in regions of the vermis and hemispheres was less extreme when *En1/En2* were ablated at ~E15 compared with at ~E13 could reflect a requirement for *En1/En2* in particular regions of the Cb between E13 and E15 (lobules IV/V in the vermis and CrusII/Paramedian in the hemispheres). However, because recombination is less efficient at the later stage with our mutagenesis system, the different phenotypes could reflect that foliation in these regions is less sensitive to lowering the dose of *En1/En2* than it is in other regions. Given the mild foliation phenotypes produced when only *En1* or *En2* is conditionally removed early compared with the extreme phenotype observed when both are reduced even at late times highlights that En function must be considered as a whole, as the two genes can compensate for each other to a large degree. However, our previous knock-in studies demonstrated that En2 has a greater capacity to regulate foliation than En1 (Sgaier et al., 2007), whereas En1 plays a dominant role in regulating parasagittal stripes of gene expression in the adult Cb (Sillitoe and Joyner, 2008).

En1/En2 regulate Cb foliation independently of Fgf8 isthmic organizer activity

Several results support a conclusion that the vermis foliation phenotype in *En1/2-E10.5* CKO mutants is not simply due to the observed reduction of *Fgf8* expression. First, different from our series of *En1/En2* CKO mutants, $Fgf8^{+/-};Fgf17^{-/-}$ mutants (Xu et al., 2000) and *Sprouty* (a negative regulator of Fgf signaling) gain-of-function mutants (Basson et al., 2008) have a specific size decrease in only anterior lobules and no relative enlargement of the central region. Thus, a reduction in Fgf8/Fgf17 signaling does not lead to global patterning changes in the vermis. Second, when *Fgf8* is conditionally ablated at ~E11 only lobules I-III are reduced in size and when ablated at ~E12 all lobules form (Sato and Joyner, 2009). Third, in mutants that lack *En1/En2* after *Fgf8* expression is terminated (~E15), lobules I-III of the vermis are nevertheless reduced in size and the relative size of the central region expanded (Fig. 3). Fourth, as in *Fgf8* conditional mutants, in *En1/2*-10.5 CKOs *Fgf17* expression is maintained at E12.5 (data not shown). Thus, a reduction in both Fgf8 and Fgf17 signaling cannot explain the defects seen in *En1/2-CKOs*. Although it is likely that *En1* and *En2* have an early function associated with Fgf8 activity in specifying the Cb and expanding the neural progenitors that give rise to the anterior vermis, they must also play a

Table 3. Summary of the times during development when conditional ablation of *En1 and/or En2* results in foliation defects

	Time gene function is ablated*				
Gene ablated	E9	E11	E12	E13	E15
En1	Yes	No	No	No	No
En2	nd	Yes	Yes	Yes	nd
En1+En2	nd	N/A	Yes	nd	Yes

*For alleles produced using Cre, time is given as 12 hours after expression of Cre; for alleles produced using CreER, time is given as 36 hours after treatment with TM (first dose when TM given twice).
N/A, not applicable, as mutants die at birth.
nd, not determined.

later role in promoting the regional diversity of Cb morphology. Interestingly, the *Drosophila engrailed* gene is required to both posteriorize the wing disc and promote growth in the posterior compartment (Guillen et al., 1995; Hidalgo, 1994).

En1/En2 regulate regional differences in gene expression and EGL thickness, as well as timing and positioning of fissures

The question arises as to how *En1/En2* regulate the pattern of foliation throughout the Cb. We found that when both En genes were conditionally ablated the stereotyped sequence of fissure formation was changed, and furthermore some fissures did not form at all, while others formed at inappropriate positions in the AP and ML axes (Fig. 8). The two most anterior fissures in the vermis formed much later than normal relative to other fissures, or did not form at all, whereas the itc fissure between lobules VI and VII in the central region formed relatively earlier. These changes in timing of fissure formation could well account for the more prominent lobules in the central region relative to the anterior-most lobules.

Significantly, in *En1/2-E10.5* CKO mutants at P2 when fissures begin to form and at P14 when foliation is nearly complete (and in the adult), lobule VI in the central region occupied a greater relative proportion of the vermis than normal and the anterior region (lobules I-V) a smaller relative proportion. Thus, *En1/En2* are involved in defining the position along the AP axis where lobules will form and the relative sizes of lobules from the onset of foliation. Moreover, three days before foliation begins in *En1/2-E10.5* mutants, the expression domains of genes that normally mark particular lobules of the vermis (AP domains) were altered in anticipation of the subsequent changes in patterning of the foliation. Interestingly, *Gli1*, which is induced in proliferating granule cells by Shh signaling from Purkinje cells, was among the genes with an altered expression pattern. Furthermore, despite the delay in foliation in mutants, the onset of Shh signaling was not delayed. Moreover, the molecular changes in granule cell precursors were accompanied by significant regional changes in the thickness of the EGL. Correlating with the increase in the relative size of the central region in *En1/2-E10.5* mutants, the normal thinning of the EGL in the central region was attenuated. The trend towards an increase in the number of proliferating cells in the anterior EGL of normal embryos also was less pronounced in *En1/2-E10.5* CKOs. Thus, the *En1/En2* genes appear to produce the distinct foliation patterns in the vermis and hemispheres by regulating spatially restricted gene expression, which leads to regional differences in the cellular processes that govern the expansion of the EGL, as well as the positioning and timing of fissure formation.

En1 and *En2* represent a new class of genes required to generate distinct foliation patterns in the vermis and hemispheres

Our study is the first to identify a gene family involved in generating the two distinct foliation patterns in the vermis and hemispheres. As En function was reduced both in dose and length of activity, the Cb progressively took on a foliation pattern with less regional diversity. The vermis phenotype did not simply result from a deletion of some of the tissue that would normally form the vermis, but instead involved a change in the relative proportions of different AP regions of the Cb, such that the anterior region was diminished and central region expanded relative to the overall size of the vermis. In addition, the three hemisphere lobules that remained in mutants did not maintain their typical morphology, and remnants of the vermis-specific anterior and posterior lobules were present more laterally than normal. It is possible that the lateral extension of vermis lobules into the hemispheres in *En1/En2* CKOs resulted from an early change in cell fate, as in $En1^{-/+};En2^{-/-}$ mutants it was found, using fate mapping, that the cells at E12.5 that normally give rise to the vermis contribute to the hemispheres as well as to the vermis (Sgaier et al., 2007).

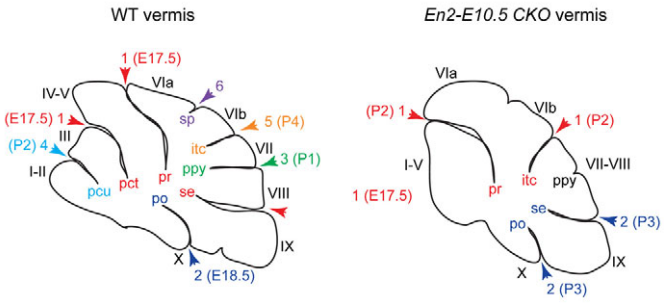

Fig. 8. Summary of the altered timing of vermis fissure formation in *En1/2-E10.5* CKOs. The order of fissure formation is color coded and indicated numerically above the arrowheads, and the times when the fissures form in the wild type (WT) and in *En1/2-E9.5* CKOs are indicated in brackets.

While an increasing number of mutations cause a decrease in the complexity of Cb foliation, the mutants to date that do not have impaired differentiation of particular cell types appear to suffer primarily depletion of the vermis or to have a foliation pattern that resembles an early developmental stage when the overall pattern is simpler. For example, removal of the transcription factor Gbx2 after E9 (Li et al., 2002), or a frame shift mutation in *Wnt1* (Thomas et al., 1991), preferentially results in reduction of the vermis. Mutations in the Fgf8 signaling pathway also affect only growth of the vermis, and preferentially the anterior vermis (Basson et al., 2008; Xu et al., 2000). In mutants such as *Meander tail*, the anterior vermis also is depleted, but as a result of abnormal differentiation (Ross et al., 1990). On the contrary, an allelic series of mutations in the Shh signaling pathway (Corrales et al., 2006), or loss of cyclin D1/D2 (Ciemerych et al., 2003), result in reduced granule cell proliferation and this leads to simplified vermis and hemisphere foliation patterns that resemble specific stages in early postnatal development. Progressive reduction in *En1/En2* function, by contrast, moves Cb morphology towards a homogeneous foliation pattern throughout the ML axis. Thus, *En1/En2* represent the first genes identified that are required to distinguish the vermis foliation pattern from that of the hemispheres. We hypothesize that *En1/En2* were co-opted during evolution to produce the morphological differences between the vermis and the hemispheres, thus providing a basis for developing additional neural circuits involving the Cb in mammals.

Acknowledgements

We are grateful to Dr P. Soriano for providing the *R26R* reporter mice and targeting constructs and Melissa Villanueva, Frada Berenshteyn and Qiuxia Guo for help with generating the targeted alleles. We thank Gina Rocco, Jason Chan, Rowena Turnbull, Julia Brandt and Nathan Turnbull for assistance with analyzing the mutants. We also thank Grant Orvis for helping to generate some of the mutants. We are grateful to Drs Sandra Blaess, Isaac Brownell, Emilie Legue, Grant D. Orvis, Praveen Raju and Roy Sillitoe for insightful comments on the manuscript and discussions. The work was supported in part by NIH grants HD050767 and MH085726 (A.L.J.), and NS038461 (D.H.T.). Deposited in PMC for release after 12 months.

Competing interests statement

The authors declare no competing financial interests.

Supplementary material

Supplementary material for this article is available at
http://dev.biologists.org/lookup/suppl/doi:10.1242/dev.027045/-/DC1

References

Altman, J. and Bayer, S. A. (1997). *Development of the Cerebellar System in Relation to its Evolution, Structure, and Functions*. New York: CRC Press.

Bai, C. B., Auerbach, W., Lee, J. S., Stephen, D. and Joyner, A. L. (2002). Gli2, but not Gli1, is required for initial Shh signaling and ectopic activation of the Shh pathway. *Development* **129**, 4753-4761.

Basson, M. A., Echevarria, D., Ahn, C. P., Sudarov, A., Joyner, A. L., Mason, I. J., Martinez, S. and Martin, G. R. (2008). Specific regions within the embryonic midbrain and cerebellum require different levels of FGF signaling during development. *Development* **135**, 889-898.

Bilovocky, N. A., Romito-DiGiacomo, R. R., Murcia, C. L., Maricich, S. M. and Herrup, K. (2003). Factors in the genetic background suppress the engrailed-1 cerebellar phenotype. *J. Neurosci.* **23**, 5105-5112.

Broccoli, V, Boncinelli, E. and Wurst, W. (1999). The caudal limit of Otx2 expression positions the isthmic organizer. *Nature* **401**, 164-168.

Chi, C. L., Martinez, S., Wurst, W. and Martin, G. R. (2003). The isthmic organizer signal FGF8 is required for cell survival in the prospective midbrain and cerebellum. *Development* **130**, 2633-2644.

Ciemerych, M. A., Kenney, A. M., Sicinska, E., Kalaszczynska, I., Bronson, R. T., Rowitch, D. H., Gardner, H. and Sicinski, P. (2002). Development of mice expressing a single D-type cyclin. *Genes Dev.* **16**, 3277-3289.

Corrales, J. D., Rocco, G. L., Blaess, S., Guo, Q. and Joyner, A. L. (2004). Spatial pattern of sonic hedgehog signaling through Gli genes during cerebellum development. *Development* **131**, 5581-5590.

Corrales, J. D., Blaess, S., Mahoney, E. M. and Joyner, A. L. (2006). The level of sonic hedgehog signaling regulates the complexity of cerebellar foliation. *Development* **133**, 1811-1821.

Crossley, P. H. and Martin, G. R. (1995). The mouse Fgf8 gene encodes a family of polypeptides and is expressed in regions that direct outgrowth and patterning in the developing embryo. *Development* **121**, 439-451.

Davis, C. A., Noble-Topham, S. E., Rossant, J. and Joyner, A. L. (1988). Expression of the homeo box-containing gene En-2 delineates a specific region of the developing mouse brain. *Genes Dev.* **2**, 361-371.

Davis, C. A., Holmyard, D. P., Millen, K. J. and Joyner, A. L. (1991). Examining pattern formation in mouse, chicken and frog embryos with an En-specific antiserum. *Development* **111**, 287-298.

Engelkamp, D., Rashbass, P., Seawright, A. and van Heyningen, V. (1999). Role of Pax6 in development of the cerebellar system. *Development* **126**, 3585-3596.

Feil, R., Wagner, J., Metzger, D. and Chambon, P. (1997). Regulation of Cre recombinase activity by mutated estrogen receptor ligand-binding domains. *Biochem. Biophys. Res. Commun.* **237**, 752-757.

Frantz, G. D., Weimann, J. M., Levin, M. E. and McConnell, S. K. (1994). Otx1 and Otx2 define layers and regions in developing cerebral cortex and cerebellum. *J. Neurosci.* **14**, 5725-5740.

Goldowitz, D. and Hamre, K. (1998). The cells and molecules that make a cerebellum. *Trends Neurosci.* **21**, 375-382.

Guillen, I., Mullor, J. L., Capdevila, J., Sanchez-Herrero, E., Morata, G. and Guerrero, I. (1995). The function of engrailed and the specification of Drosophila wing pattern. *Development* **121**, 3447-3456.

Hanks, M., Wurst, W., Anson-Cartwright, L., Auerbach, A. B. and Joyner, A. L. (1995). Rescue of the En-1 mutant phenotype by replacement of En-1 with En-2. *Science* **269**, 679-682.

Hidalgo, A. (1994). Three distinct roles for the engrailed gene in Drosophila wing development. *Curr. Biol.* **4**, 1087-1098.

Indra, A. K., Warot, X., Brocard, J., Bornert, J. M., Xiao, J. H., Chambon, P. and Metzger, D. (1999). Temporally-controlled site-specific mutagenesis in the basal layer of the epidermis: comparison of the recombinase activity of the tamoxifen-inducible Cre-ER(T) and Cre-ER(T2) recombinases. *Nucleic Acids Res.* **27**, 4324-4327.

Inouye, M. and Oda, S. I. (1980). Strain-specific variations in the folial pattern of the mouse cerebellum. *J. Comp. Neurol.* **190**, 357-362.

Johnson, G. A., Cofer, G. P., Fubara, B., Gewalt, S. L., Hedlund, L. W. and Maronpot, R. R. (2002). Magnetic resonance histology for morphologic phenotyping. *J. Magn. Reson. Imaging* **16**, 423-429.

Joyner, A. L. and Martin, G. R. (1987). En-1 and En-2, two mouse genes with sequence homology to the Drosophila engrailed gene: expression during embryogenesis. *Genes Dev.* **1**, 29-38.

Joyner, A. L., Herrup, K., Auerbach, B. A., Davis, C. A. and Rossant, J. (1991). Subtle cerebellar phenotype in mice homozygous for a targeted deletion of the En-2 homeobox. *Science* **251**, 1239-1243.

Larsell, O. (1970). *The Comparative Anatomy and Histology of the Cerebellum from Monotremes through Apes* (ed. J. Jansen), pp. 31-58. Minneapolis, MN: University of Minnesota Press.

Lewis, P. M., Gritli-Linde, A., Smeyne, R., Kottmann, A. and McMahon, A. P. (2004). Sonic hedgehog signaling is required for expansion of granule neuron precursors and patterning of the mouse cerebellum. *Dev. Biol.* **270**, 393-410.

Li, J. Y., Lao, Z. and Joyner, A. L. (2002). Changing requirements for Gbx2 in development of the cerebellum and maintenance of the mid/hindbrain organizer. *Neuron* **36**, 31-43.

Liu, A. and Joyner, A. L. (2001). EN and GBX2 play essential roles downstream of FGF8 in patterning the mouse mid/hindbrain region. *Development* **128**, 181-191.

Lauder, J. M., Altman, J. and Krebs, H. (1974). Some mechanisms of cerebellar foliation: effects of early hypo- and hyperthyroidism. *Brain Res.* **76**, 33-40.

MacLeod, C. E., Zillesb, K., Schleicherb, A., Rillingd, J. K. and Gibson, K. R. (2003). Expansion of the neocerebellum in Hominoidea. *J. Hum. Evol.* **44**, 401-429.

Matise, M. P., Auerbach, W. and Joyner, A. L. (2000). Production of targeted embryonic stem cell clones. In *Gene Targeting* (ed. B. D. Hames), pp. 101-132. Oxford: Oxford University Press.

Millen, K. J., Hui, C. C. and Joyner, A. L. (1995). A role for En-2 and other murine homologues of Drosophila segment polarity genes in regulating positional information in the developing cerebellum. *Development* **121**, 3935-3945.

Purves, D., Augustine, G. J., Fitzpatrick, D., Hall, W. C., LaMantia, A., MaNamara, J. O. and Williams, S. M. (eds) (2004). *Neuroscience*, 3rd edn. Sunderland: Sinauer Associates.

Rodriguez, C. I., Buchholz, F., Galloway, J., Sequerra, R., Kasper, J., Ayala, R., Stewart, A. F. and Dymecki, S. M. (2000). High-efficiency deleter mice show that FLPe is an alternative to Cre-loxP. *Nat. Genet.* **25**, 139-140.

Ross, M. E., Fletcher, C., Mason, C. A., Hatten, M. E. and Heintz, N. (1990). Meander tail reveals a discrete developmental unit in the mouse cerebellum. *Proc. Natl. Acad. Sci. USA* **87**, 4189-4192.

Sato, T. and Joyner, A. L. (2009). Duration of *Fgf8* isthmic organizer expression is key to patterning different tectal-isthmo-cerebellum structures. *Development* **136**, 3617-3626.

Sgaier, S. K., Millet, S., Villanueva, M. P., Berenshteyn, F., Song, C. and Joyner, A. L. (2005). Morphogenetic and cellular movements that shape the mouse cerebellum; insights from genetic fate mapping. *Neuron* **45**, 27-40.

Sgaier, S. K., Lao, Z., Villanueva, M. P., Berenshteyn, F., Stephen, D., Turnbull, R. K. and Joyner, A. L. (2007). Genetic subdivision of the tectum and cerebellum into functionally related regions based on differential sensitivity to engrailed proteins. *Development* **134**, 2325-2335.

Shirasawa, S., Arata, A., Onimaru, H., Roth, K. A., Brown, G. A., Horning, S., Arata, S., Okumura, K., Sasazuki, T. and Korsmeyer, S. J. (2000). Rnx deficiency results in congenital central hypoventilation. *Nat. Genet.* **24**, 287-290.

Sillitoe, R. V. and Joyner, A. L. (2007). Morphology, molecular codes, and circuitry produce the three-dimensional complexity of the cerebellum. *Annu. Rev. Cell Dev. Biol.* **23**, 549-577.

Sillitoe, R. V., Stephen, D., Lao, Z. and Joyner, A. L. (2008). *Engrailed* homeobox genes determine the organization of Purkinje cell sagittal stripe gene expression in the adult cerebellum. *J. Neurosci.* **28**, 12150-12162.

Soriano, P. (1999). Generalized lacZ expression with the ROSA26 Cre reporter strain. *Nat. Genet.* **21**, 70-71.

Sudarov, A. and Joyner, A. L. (2007). Cerebellum morphogenesis: the foliation pattern is orchestrated by multi-cellular anchoring centers. *Neural Develop.* **2**, 26.

Thomas, K. R., Musci, T. S., Neumann, P. E. and Capecchi, M. R. (1991). Swaying is a mutant allele of the proto-oncogene Wnt-1. *Cell* **67**, 969-976.

Wurst, W., Auerbach, A. B. and Joyner, A. L. (1994). Multiple developmental defects in Engrailed-1 mutant mice: an early mid-hindbrain deletion and patterning defects in forelimbs and sternum. *Development* **120**, 2065-2075.

Xu, J., Liu, Z. and Ornitz, D. M. (2000). Temporal and spatial gradients of Fgf8 and Fgf17 regulate proliferation and differentiation of midline cerebellar structures. *Development* **127**, 1833-1843.

Zambrowicz, B. P., Imamoto, A., Fiering, S., Herzenberg, L. A., Kerr, W. G. and Soriano, P. (1997). Disruption of overlapping transcripts in the ROSA beta geo 26 gene trap strain leads to widespread expression of beta-galactosidase in mouse embryos and hematopoietic cells. *Proc. Natl. Acad. Sci. USA* **94**, 3789-3794.